Choosing Your Tools©

Bruce E. Brinson*, Rice University
Marie Pontier-Johnson, Continental Carbon Company
*brinson@rice.edu

The increasing availability of the user-friendly black box can present an increased probability of characterization errors. The uninformed choice (*e.g.*, any SEM will see this) or dependence on one instrument can also lead to erroneous results. Failure to understand the limits and advantages of a particular instrument and bias through assumption or desired result can be equally deceptive.

In the example presented here, the objectives are to determine primary particle size and to identify the impurities in a specimen. We will look at the data produced by several instruments and discuss the ways each technology can support or mislead the analysts.

Images were acquired optically by secondary electron (SE), x-ray dot maps and back scattering electrons (BSE). The elemental analysis techniques used were Energy Dispersive Spectrometry (EDS), Wavelength Dispersive Spectrometry (WDS) and Powder x-ray diffractometry (PXD).

Field emission SEM (FESEM) and optical images are used. A comparison will be made between the apparent grain size observed optically, in the μ-probe and grain size(s) derived from x-ray data via the Scherrer Formula. Ductile fracture at grain boundaries will also be shown and discussed.

A PXD scan, recorded in an attempt to qualitatively identify elements present, will demonstrate the difficulty in resolving certain combinations of elements. Suspected contaminates are Cr, Ni, Al, W, Cu, Si and Ag.

EXPERIMENTAL

Sample Preparation: The specimen was made from gold vacuum system gaskets (~20 g) and foils/films (~5 g) from a resistively heated thin film deposition system. The material was melted by direct flame, cast into a bar and cooled at room temperature. There was no additional annealing. It has been determined to be 22 karat gold by an acid litmus test common to the jewelry industry. For fracture images, the bar was thinned by compression with a wire-cutting tool and broken apart by repetitive flexing. Sample preparation was limited to cleaning with methanol prior to analysis and imaging. Elemental analysis was performed on a broad surface of the bar.

Micro Probe experimental parameters: EDS and WDS data were collected at 15 kV, 15 nA with a spot size of 10 μm. The scan dwell times and step sizes are as follows: EDS = 50 sec and WDS = 1000 msec/step. The PAP[5] method for matrix corrections was used. Spectrometer crystals were: LIF, d = 4.03 Å, PET, d = 8.75 Å, TAP, d = 25.745 Å and PC1, d = 61.5 Å, where d is the known crystallographic spacing.

PXD experimental parameters: 20 kV, 20 mA, λ=1.54 Å (CuKα), x-ray slit = 0.4 mm, detector slit = 0.3 mm, scan range is 2θ = 20 - 40°; step size = 0.05°, scan range is 2θ = 40-80° step size = 0.02°, dwell time = 20 sec. A nickel filter was used to attenuate CuK$_β$ radiation.

RESULTS and DISCUSSION

PXD: Our specimen is not a powder but in bar form. The peak intensities could be skewed by preferential grain orientation. With this constraint only qualitative interpretations can be made. Gold can account for all major peaks (Figure1). Minor peaks appear to be the results of CuK$_β$ radiation passing through the Ni filter. An example is found at 2θ = 34.4°. None

of the suspected contaminates account for that peak or 7 other peaks found by expanding the y-axis (not shown).

In a predominately Au specimen, arguments for Ag peaks are completely lost in the Au peaks. Silver and gold have the same symmetry, [face centered cubic (fcc), where a = 4.07 Å][4], crystal structure and lattice parameters. Two Cr peaks in the scanned range also coincide. If the scan had extended past 2θ = 80°, a Cr at peak at 81.72° would have been seen. If Cr is present, this obtainable data point was lost to operator ignorance. Weak arguments for aluminum, also fcc, could be made but without prior knowledge would and probably should go completely unnoticed. That prior or assumed knowledge present a bias to the experimentalist as will be shown. If in significant fractional quantity, the Al peaks would be resolvable in the wings of the Au peaks. Aluminum was believed to be the most probable impurity from the deposition system.

Copper peaks were not observed, we will find the sample to be ~3% Cu (atomic wt. percent). In a review of Au$_n$Cu$_m$ compounds[2] only Bogdanovite (Au$_3$Cu) has been identified with major peaks that could be obscured by the pure Au peaks. Bogdanovite also has a number of minor peaks but the significant indication is a slight shift in the (220) peak. We do not see the minor peaks or the (220) peak shift. It is worth noting that our x-ray source uses a Cu target. The Cu$_K$ absorption peak at 8.98 keV will heavily attenuate the incident 8.0 keV x-ray radiation. For a material suspected to be only ~ 90% pure this technique is deceptive. PXD leads us to believe it is pure gold.

The peak width in our x-ray data provides us with data by which we can make a reasonable approximation of crystal size. The Scherrer[1] formula is used to make the grain size calculations. By the Scherrer formula the typical gold grain size is found to be ~28 nm (x, y, z).

$$T = 0.9\lambda/B * Cos\theta_B \qquad \text{Eq. 1}$$

where B in radians = FWHM or $(2\theta_2 - 2\theta_1)/2$

$\theta_B = w = 2\theta/2$, $\lambda_{Cu} = 1.54$Å

This is substantially smaller than the apparent grain size of 5-10 μm as seen in Figure 4. These spheroid structures are actually gold aggregates. Close inspection of Figure 2, an FESEM image, shows anhedral nano scale crystals about a triple point of 5-10 μm scale aggregates. Further support of the aggregate nature is found at the far right of this image where we see two triple points within the ~10 μ feature.
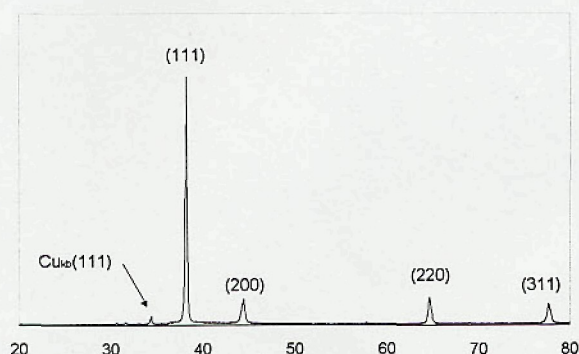

Figure 1   Powder X-ray spectra showing only gold peaks. The peak labeled Cu$_{KB}$ (111) is the Au (111) peak produced by Cu$_{Kb}$ radiation (1.39Å).

Choosing Your Tools
Continued from page 26

Figure 2: Field emission SEM image showing triple points & anhedral nano scale crystals.
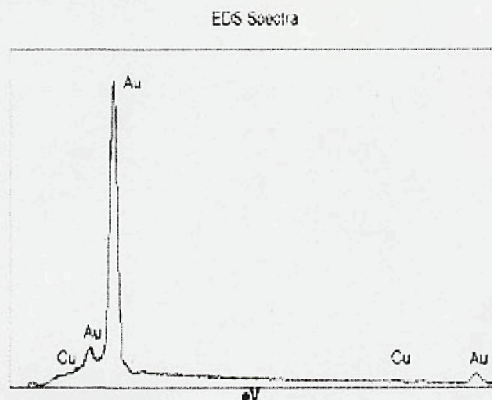

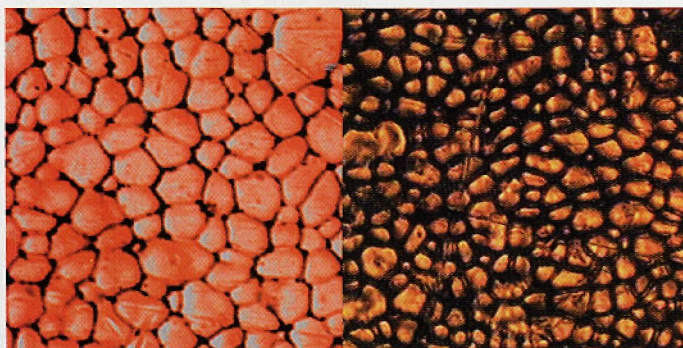Figure 3: EDS spectra of the specimen showing gold & copper peaks.

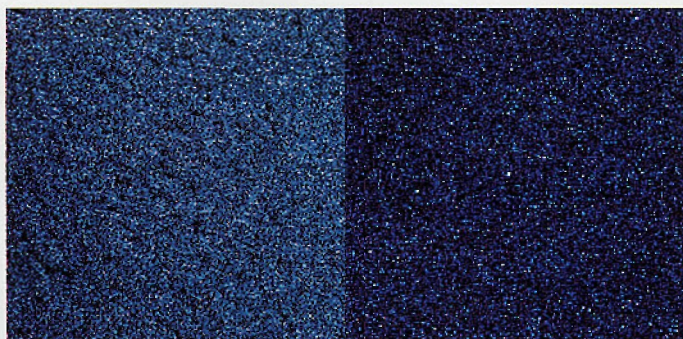Figure 4: Au Specimen, BSE image (left), Optical (right)

Figure 5: WDS X-Ray maps of the area shown in the BSE image in Figure 4 indicating a uniform distribution of gold (left) and copper (right) in the specimen.

X-Ray ANALYTICAL MICROSCOPY: EDS and WDS

The qualitative EDS scan (Figure3) indicates only Au and Cu. The Cu (assumed previous knowledge) had a low probability, in the author's opinion, of being present, but is in fact the only other viable peak. Expansion of the y-axis (not shown) was required to observe the Cu peaks.

A qualitative WDS scan for all elements confirmed the Au-Cu combination. The Au and Cu peaks are well-defined as shown in Figure 6. In addition to the LIF and PC1 crystals, scans using TAP and PET crystals were acquired (data not shown) to complete the search for all elements. All other elements were eliminated. Interestingly, the LIF scan shows a peak in the vanadium ($V_{K\alpha}$) position, but no supporting peaks were observed in any of the spectra, leaving the author hesitant to make a claim for vanadium. Three spurious peaks (Figure 6) remain in question but were evaluated up to 5th diffraction order without a conclusive result. TAP and PET scans were found to include only higher order Au and Cu peaks. Figure 7 shows oxygen suggesting the presence of a copper oxide. In the right upper corner of (FESEM image) Figure 8 is a feature recognized by the author as similar to oxidized copper.

The copper content is ~3.1% (atomic) as determined by WDS. The deviation was ±0.3% indicating some non-homogeneity on the 10 μm scale, but x-ray dot maps in Figure 5 suggest in general we have uniform Cu distribution. An inadequate surface polishing may result in increased experimental error. The dot maps in Figure 5 correlate to the BSE image in Figure 4.

IMAGING MICROSCOPY: The nominal aggregate size is 5-10 μm. This is observed in the BSE and optical images found in Figure 4 and SE images in Figure 2. Examination of the left-hand images in Figure 8 shows that the material fractured at the aggregate boundaries. Without knowing that spheroids seen in the μ-probe images are actually polycrystalline aggregates, one might
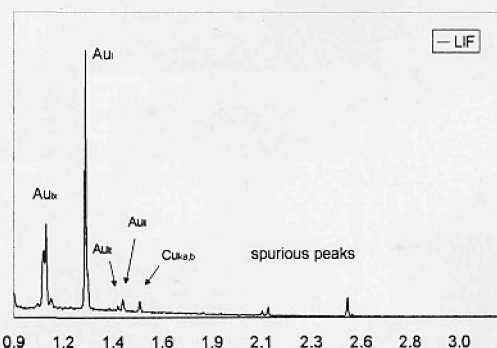

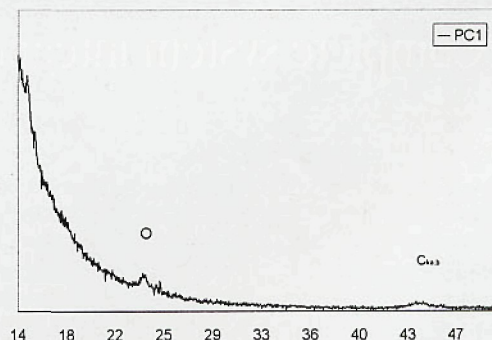Figure 6: WDS scan showing gold, copper and spurious peaks. Horizontal units are in angstroms (Å).

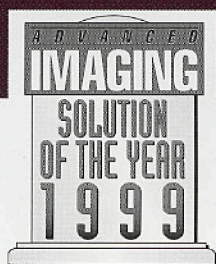Figure 7: WDS scan clearly showing an oxygen peak. Horizontal units are in angstroms (Å).
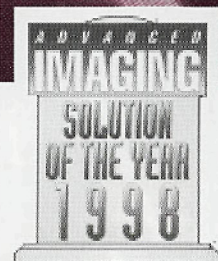
Choosing Your Tools
Continued from page 28

draw the conclusion from PXD data that the failure is associated with the nanoscale grains, where in fact it appears to fail at aggregate boundaries. The crystallite size indicated by PXD and imaged by FESEM are not significant in the failure, *i.e.*, it is a ductile failure not catastrophic.

DISCUSSION AND CONCLUSION

Of the chosen instruments, none of them alone would provide a correct analysis. Yet, for 2 of the 3 techniques it would be easy to believe the solutions were complete and correct. The PXD gave the approximate crystal or grain size by the Scherre equation. PXD provides crystallographic spacings (d) but cannot discriminate between gold and several metals. The FESEM is an excellent imaging tool but does not have analytical capability. It gives a visual conformation of the nanoscale crystals predicted by the Scherrer formula. It also nicely resolves the details of the fracture surface and triple points between and within aggregates. It should note that "grains" are presumed to be single crystals in a polycrystalline material. In a secondary electron or optical image the various orientations of grains can provide a contrast mechanism (both in gray scale and texture) that can allow for the observation of grain boundaries.

In many cases special surface preparations are required. The High Resolution FESEM image (Figure 2) shows uniformity in the gray scale and texture suggesting the isotropic nature of the ~10 µm structures, *i.e.,* they are aggregates. The FESEM also allows us to visualize that fracturing will occur at aggregate boundaries, not grain or crystallographic boundar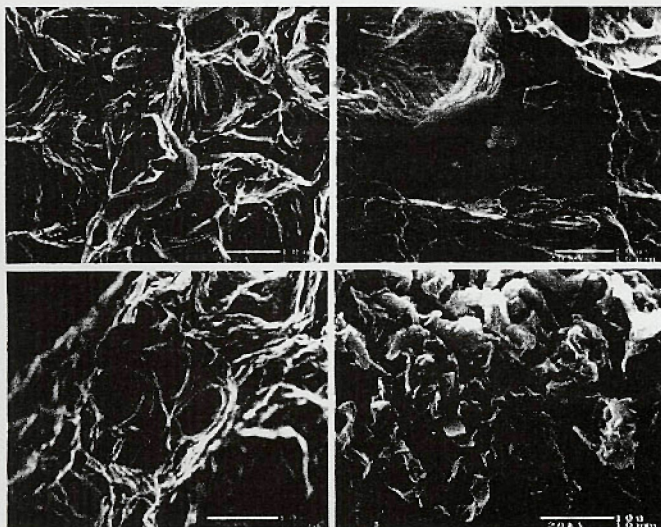ies. The detail seen in these FESEM images are observable because this instrument is optimized for high-resolution imaging.

The hardware configuration differs between high-resolution imaging and analytical SEMs. For analytical work, *e.g.,* x-ray spectrometry, secondary electron imaging resolution is sacrificed for higher beam currents and electron emission stability. This is done to improve the signal statistics of their respective detection systems.

The EPMA (electron probe microanalysis or µ-Probe) EDS qualifies the presence of Cu to the trained eye, but WDS truly confirms and quantifies that which PXD could not - the presence of Cu. WDS also indicates oxygen, suggesting the presence of Cu_2O or CuO support by FESEM and the analyst's previous experience. Even with the WDS data on oxygen, making the claim that an oxide is present based on past experience and an SE image (Figure 8) is only an informed opinion.

The BSE image does not suggest the presence of nanocrystal gold grains for 2 reasons: 1) As an analytical platform, the µ-probe is designed to get many of electrons to the specimen. This necessitates the use of larger aperture optics and thus a concession in probe size and resolution. In this case, the minimum electron beam size at the specimen is larger than the nanoscale features. 2) Unlike the secondary electron signal intensity, which is highly dependent on the angle of incidence ($\delta(\theta)=\delta o SEC\theta$), backscatter electron coefficients are dependent on the element.[3] With these two constraints, the fine details are not to be seen.

This data has shown with a seemingly simple sample that in this age of automated, easy-to-use black boxes, the potential for error is not negligible. Likewise, assumptions, desires and assumed properties can easily lead the researcher to erroneous conclusions.

To the research student or scientist choosing your tools means choosing tools that you understand well. ■

Figure 8: FESEM images of the specimen showing morphologies in the fracture zone. Scale bar =10 µm. Left upper and lower FESEM images show ductile parting of grains. The right upper image shows a feature of lower secondary emission and a decisively different form. In the authors experience it is similar to copper oxide but elemental analysis was not available. The lower right image shows distinct features that are much smaller than our typical aggregate. This area was in contact with the beveled surface of the cutting device used to thin the sample before cold-working to fracture the sample. This is probably a form of extrusion. Again the Au crystals are significantly smaller the ribbon like features.

References
1. Elements of X-Ray Diffraction 2nd ed., B. D. Cullity, Addison-Wesley Publishing Co, ISBN 0-201-01174-3.
2. International Center for Diffraction Data, 1993 Release A6.
3. Scanning Electron Microscopy and X-ray Microanalysis, Goldstein *et. al.*, p. 111 Plenum Press ISBN 0-306-44175-6.
4. Hand book of Chemistry and Physics, p. E-204, CRC Press Inc. ISBN 0-8493-0460-8.
5. Electron Microprobe Analysis, 2nd. Ed., S. J. B. Reed, p. 32, p. 153-4, Cambridge University press, ISBN 0-521-59944-X.

SPI SUPPLIES

File   Edit   View   Go   Bookmarks   Options   Directory   Help

Netscape: Structure Probe, Inc.

| Back | Forward | Home | Reload | Images | Open | Print | Find | Stop | N |

| What's New? | What's Cool? | Handbook | Net Search | Net Directory | Newsgroups |

Welcome to STRUCTURE PROBE, INC.
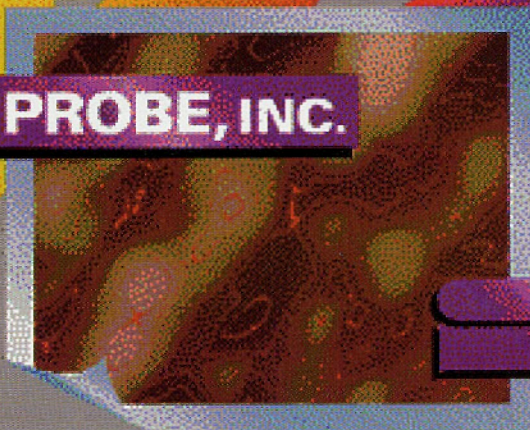
spi SUPPLIES

Discover The SourceBook Online
http://www.2spi.com
Up-To-The-Minute Information
For All Your Microscopy Needs

SPI Supplies Division of **STRUCTURE PROBE, Inc.**
P.O. Box 656 • West Chester, PA 19381-0656 USA
Ph.: 1-610-436-5400 • 1-800-2424-SPI (U.S. only) • **FAX:** 1-610-436-5755 • **E-mail:** spi2spi@2spi.com